Confined Brownian ratchets

Paolo Malgaretti, Ignacio Pagonabarraga, and J. Miguel Rubi

Additional information on J. Chem. Phys.

Confined Brownian ratchets

Paolo Malgaretti,[a)] Ignacio Pagonabarraga, and J. Miguel Rubi

Department de Fisica Fonamental, Universitat de Barcelona, 08028 Barcelona, Spain

We analyze the dynamics of Brownian ratchets in a confined environment. The motion of the particles is described by a Fick-Jakobs kinetic equation in which the presence of boundaries is modeled by means of an entropic potential. The cases of a flashing ratchet, a two-state model, and a ratchet under the influence of a temperature gradient are analyzed in detail. We show the emergence of a strong cooperativity between the inherent rectification of the ratchet mechanism and the entropic bias of the fluctuations caused by spatial confinement. Net particle transport may take place in situations where none of those mechanisms leads to rectification when acting individually. The combined rectification mechanisms may lead to bidirectional transport and to new routes to segregation phenomena. Confined Brownian ratchets could be used to control transport in mesostructures and to engineer new and more efficient devices for transport at the nanoscale. © *2013 AIP Publishing LLC*. [http://dx.doi.org/10.1063/1.4804632]

I. INTRODUCTION

Breaking detailed balance due to the presence of unbalanced forces acting on a system causes rectification of thermal fluctuations and leads to new dynamical behaviors, very different from those observed in equilibrium situations.[1, 2] Typical realizations of rectified motion include the transport of particles under the action of unbiased forces of optical,[3,4] mechanical,[5,6] or chemical[7,8] origin. Hence, the implications of rectification has attracted the interest of researchers in a variety of fields, ranging from biology to nanoscience, due to its relevance in the transport and motion at small scales.[2,9] Accordingly, the behavior of such small engines, referred to as Brownian ratchets, have been deeply studied and several models that capture some of their main features have been proposed.[1,2,10,11]

Given the small size of rectifying elements, it is likely that their motion takes place close to boundaries or in confined environments. Nevertheless, ratchet models usually assume that rectification develops in an unbound medium. Since rectification develops as an interplay associated to how a particle experiences local forces while it explores the space around it, confinement plays an important role because it significantly reduces the number of allowed states of the rectifying elements. This restriction can be understood as an effective change of the entropy of the Brownian ratchet as it displaces along the confined environment.[12]

The relevance of entropic barriers to promote entropic transport[13,14] in confined environments has been recognized in a variety of situations that include molecular transport in zeolites,[15] ionic channels,[16] or in microfluidic devices,[17,18] where their shape explains, for example, the magnitude of the rectifying electric signal observed experimentally.[19] In fact, spatially varying geometric constraints provide themselves an alternative means to rectify thermal fluctuations.[12]

Modulations in the available explored region lead to gradients in the system effective free energy, by inducing a local bias in its diffusion that can promote a macroscopic net velocity for aperiodic channel profiles[12] or due to applied alternating fields.[20]

We will analyze the interplay between rectification and confinement, and will characterize the new features associated to confined Brownian ratchets (CBR). We show that the presence of strong cooperative rectification[21] between the ratchet and the geometrical confinement may lead to rectification even when none of them can rectify the particle current on their own. Such an interplay strongly affects particle motion. To understand the mutual influence between both rectifying sources, we will analyze three different ratchet models, namely, the flashing ratchet, the two-level ratchet, and a thermal ratchet. In the first two cases, the equilibrium is broken by the energy injected in the system through the intrinsic ratchet mechanism as it happens in the case of molecular motors. In the third one, the driving force is a thermal gradient that couples to the probability current, hence inducing a, local, Soret effect.

The article is distributed as follows. In Sec. II, we present the main features of entropic transport and formulate the kinetic framework, based on the Fick-Jacobs equation, that will allow us to describe the evolution of the probability distribution of a particle in the presence of free energy barriers. The ratchet models that will be analyzed in detail are described in Sec. III. In Secs. IV– VII we discuss the different scenarios generated by different symmetric/asymmetric ratchets and/or channel shapes, and conclude in Sec. VIII where we draw the main conclusions and outlook of this piece of work.

II. PARTICLE DYNAMICS IN A CONFINED MEDIUM

A Brownian ratchet, with diffusion constant D, under the action of a potential, $V(\mathbf{r}, t)$, moving in a confined environment characterized by a varying cross-section channel

---

a)Author to whom correspondence should be addressed. Electronic mail: paolomalgaretti@ffn.ub.es
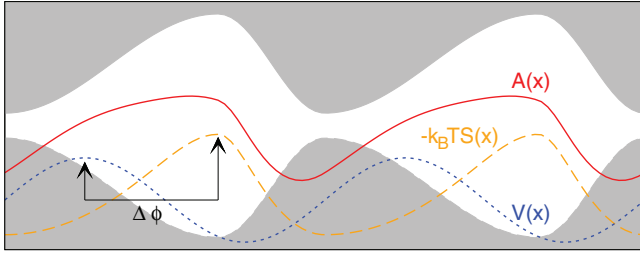
FIG. 1. Brownian ratchet and entropic barriers. A Brownian motor moving in a confined environment will be sensitive to the free energy $A(x)$ (solid) generated by the ratchet potential $V(x)$ (dotted) and the entropic potential (dashed), $-k_BTS(x)$, induced by the channel shape.

of width, $h(x, z)$, such as the one depicted in Fig. 1, can be characterized in terms of the probability distribution function (pdf), $P(\mathbf{r}, t)$, which obeys the Smoluchowsky equation,

$$\frac{\partial}{\partial t} P(\mathbf{r}, t) = \nabla \cdot [\beta D \nabla W(\mathbf{r}) P(\mathbf{r}, t) + D \nabla P(\mathbf{r}, t)], \quad (1)$$

where $\beta^{-1} = k_BT$ is the inverse of the temperature, T, at which the particle diffuses, while k_B stands for Boltzmann constant. Instead of being regarded as an explicit boundary condition, the geometrical constraint can be included, alongside any additional potential the diffusing particle may be subject to, as an effective potential

$$W(\mathbf{r}) = \begin{cases} V(x), & |y| \leq h(x), \, \& \, |z| \leq L_z, \\ \infty, & |y| > h(x) \, \text{or} \, |z| > L_z, \end{cases} \quad (2)$$

where we have considered, without lack of generality, that the long axis of the channel coincides with the axis x, that particles cannot penetrate the confining channel walls, and that the channel is periodic, $W(\mathbf{r}) = W(\mathbf{r} + L\mathbf{e}_x)$, of length L, as shown in Fig. 1, and has a finite section. If the channel width varies slowly, $\partial_x h \ll 1$, one can assume that the particle equilibrates in the transverse section on time scales smaller than the ones in which the particle experiences the variations in channel section. It is then possible to factorize the pdf

$$P(\mathbf{r}, t) = p(x, t) \frac{e^{-\beta W(\mathbf{r})}}{e^{-\beta A(x)}}, \quad (3)$$

$$e^{-\beta A(x)} = \int_{-L_z}^{L_z} \int_{-h(x)}^{h(x)} e^{-\beta W(\mathbf{r})} dy \, dz. \quad (4)$$

By integration over the channel section one arrives at

$$\frac{\partial}{\partial t} p(x, t) = \partial_x \{D[\beta p(x, t) \partial_x A(x) + \partial_x p(x, t)]\}, \quad (5)$$

the Fick-Jacobs equation,[22–24] an effective one-dimensional Smoluchowsky equation that determines the particle diffusion along the channel. Such motion is characterized by the local effective free energy

$$A(x) = V(x) - k_BT \ln[2h(x)], \quad (6)$$

where $S(x) = \ln(2h(x))$ accounts for the entropic contribution due to confinement. One can identify an entropy barrier,

$$\Delta S = \ln\left(\frac{h_{max}}{h_{min}}\right) \quad (7)$$

in terms of the maximum, h_{max}, and minimum, h_{min} channel apertures. Therefore, $\partial_x A(x)$ is the driving force that contains entropic, $\partial_x S(x)$, and enthalpic, $\partial_x V(x)$, contributions. The range of validity of the Fick-Jacobs equation has been analyzed,[13,25] and it has been found that introducing the varying diffusion coefficient[24]

$$D(x) = \frac{D_0}{\left[1 + \left(\frac{\partial h}{\partial x}\right)^2\right]^\alpha} \quad (8)$$

with $\alpha = 1/3, 1/2$ for 3D, 2D, respectively, with the reference diffusion $D_0 = k_BT/\gamma(R)$ and $\gamma(R) \propto R$, enhances the range of validity of the factorization assumption, Eq. (4). Although we will keep $D(x)$ for completeness, the results do not change qualitatively if a constant diffusion coefficient, D_0, is considered instead.

The free energy difference over a channel period

$$\Delta F = \int_0^L \partial_x A(x) dx \quad (9)$$

governs the particle current onset. Looking for the steady solution of Eq. (5) in a periodic system, $p_{st}(0) = p_{st}(L)$, we find that a net current, $J \neq 0$, arises only when $\Delta F \neq 0$, which can have both an enthalpic, $\int_0^L V(x) dx \neq 0$, and entropic, $k_BT \int_0^L \ln(h(x)) dx \neq 0$, origin. Indeed the picture of $A(x)$ as a free energy is suggestive: a net current sets only when the difference in free energy along the period is not vanishing. Clearly, at equilibrium, periodic potentials, $V(x)$, in periodic channels, $h(x)$, do not give rise to any difference in the free energy and consequently no current. The relative performance of a ratchet in an uniform channel can be quantified in terms of the dimensionless parameter,

$$\mu_0 = \frac{L v_0}{\tilde{\mu} \Delta F_0}, \quad (10)$$

defined as the ratio between the Brownian ratchet average speed, $\bar{v} = \frac{1}{L} \int_0^L J(x) dx$ with $J(x) = D[\beta p(x, t) \partial_x A(x) + \partial_x p(x, t)]$ derived from Eq. (5), and the average speed of a particle with mobility $\tilde{\mu} \equiv \beta D_0$ under the action of a uniform effective force, $f_0 \equiv \Delta F_0/L$. In the absence of intrinsic ratchet rectification, $\Delta F_0 = 0$ and μ_0 remains 1. If the ratchet leads to an intrinsic rectification, the interplay between ratcheting and confinement can be alternatively quantified in terms of the dimensionless parameter

$$\mu = \frac{L \bar{v}}{\tilde{\mu} \Delta F} \quad (11)$$

that accounts for the overall free energy drop ΔF. For a uniform channel, when rectification is purely enthalpic, $\mu/\mu_0 = 1$. Therefore, deviations of μ/μ_0 from 1 constitute a convenient means to address the role of entropic constraints to particle rectification; $\mu/\mu_0 > 1$ indicates that the geometrical constraints cooperate with the force associated to the Brownian ratchet to induce an efficient cooperative rectification, larger than the one obtained in an unstructured environment, while the opposite holds for $\mu/\mu_0 < 1$. The absolute value of μ gives additional information. On one hand, when $\mu > 1$ the performance of the cooperative rectification beats the one obtained under a constant force $f \equiv \Delta F/L$, on the other hand,

μ also easily identifies the nonlinear rectifying regime, when $\partial_f \mu \neq 0$.

To analyze the interplay between the Brownian ratchet and confinement, we will consider that all Brownian ratchets are subject to the same underlying, driving periodic potential,

$$V_0(\mathbf{r}) = V_0 \left[\sin \frac{2\pi}{L} x + \lambda \sin \frac{4\pi}{L} x \right]. \qquad (12)$$

This is a simple potential, explored in detail previously in which rectification is controlled by a single parameter, λ.[26] We will consider a channel width that varies with the same periodicity as V_0 and with a similar functional dependence

$$h(x) = h_0 - R + h_1 \sin \left[\frac{2\pi}{L}(x + \phi_0) \right] + h_2 \sin \left[\frac{4\pi}{L}(x + \phi_0) \right], \qquad (13)$$

where h_0 is the average channel section and h_1 and h_2 determine its modulation. In particular h_2 is responsible for the symmetry of the channel along its transverse axis. When $h_2 \neq 0$ the left-right symmetry along the channel longitudinal axis is broken while, for $h_2 = 0$, the left-right symmetry of channel along its longitudinal axis is restored. h_{max} and h_{min} depend both on h_1 and h_2 and the dephasing, ϕ_0. The latter will be useful to displace the geometrical and potential modulations, as discussed in Secs. IV–VII. The particle radius, R, affects the available transverse section and will hence contribute to the entropic barrier, Eq. (7).

III. RATCHET MODELS

In order to analyze the impact of confinement in the rectification of a Brownian particle, we will consider three different types of complementary, well-established ratchet models that have the same periodicity that the geometric confinement.

A. Flashing ratchet

A colloidal particle subjected to a periodic external potential

$$V(x) = \mathcal{V}_1 V_0(x) \qquad (14)$$

behaves as a flashing ratchet when the random force breaks detailed balance.[4] This can be simply achieved for a Gaussian white noise with a second moment amplitude $g(x) = \sqrt{D(x) + Q(\partial_x V_0(x))^2}$,[11] where Q controls Brownian rectification. The Fick-Jacobs equation for such a flashing ratchet in a varying-section channel reads

$$\frac{\partial}{\partial t} p(x) = \frac{\partial}{\partial x} \left\{ g(x) \frac{\partial[p(x)g(x)]}{\partial x} + D(x)p(x) \frac{\partial \beta A(x)}{\partial x} \right\}, \qquad (15)$$

which reduces to equilibrium diffusion for $Q = 0$. For $Q > 0$ detailed balance is broken and net fluxes arise when

$$\beta \Delta F = \int_0^L \left[\frac{D(x)\partial_x A(x)}{g(x)^2} + \frac{\partial}{\partial x} \ln g(x) \right] dx \neq 0. \qquad (16)$$

Since $\int_0^L \partial_x \ln g(x) dx = 0$ for a periodic channel, particle currents emerge from the interplay between both the en-

tropic and enthalpic forces, encoded in $A(x)$ and the position-dependent noise, $g(x)$. Three dimensionless parameters governs the Brownian ratchet performance: $\beta \mathcal{V}_1$ and ΔS quantify the relevance of the enthalpic and entropic contributions, respectively, while $Q/(L^2 D_0(R))$ determines rectification.

B. Two state molecular motor

The two-state ratchet model constitutes a standard, simple framework to describe molecular motor motion. A Brownian particle jumps between two states, $i = 1, 2$, (strongly and weakly bound) that determine under which potential, $V_{i=1,2}$, it displaces.[10] A choice of the jumping rates $\omega_{12, 21}$ that break detailed balance, jointly with an asymmetric potential of the bound sate, $V_1(x)$, determines the average molecular motor velocity $v_0 \neq 0$. The conformational changes of the molecular motors introduce an additional scale that will compete with rectification and geometrical confinement. Infinitely processive molecular motors remain always attached to the filament along which they displace and are affected by the geometrical restrictions only while displacing along the filament; accordingly, we choose channel-independent binding rates $\omega_{21, p}(x) = k_{21}$. On the contrary, highly non-processive molecular motors detach frequently from the biofilament and diffuse away; an effect we account for considering a channel-driven binding rate, $\omega_{21, np}(x) = k_{21}/h(x)$. Motors jump to the weakly bound state only in a region of width δ around the minima of $V_1(x)$, with rate $\omega_{12} = k_{12}$. Accordingly, the motor densities in the strong(weak) states, $p_{1(2)}$ along the channel follow[10]

$$\partial_t p_1(x) + \partial_x J_1 = -\omega_{12}(x)p_1(x) + \omega_{21}(x)p_2(x),$$
$$\partial_t p_2(x) + \partial_x J_2 = \omega_{12}(x)p_1(x) - \omega_{21}(x)p_2(x), \qquad (17)$$

where $J_{1, 2}(x) = -D(x)[\partial_x p_{1, 2}(x) + p_{1, 2}(x)\partial_x \beta A_{1, 2}(x)]$ stands for the current densities in each of the two states in which motor displaces. Depending on the motor internal state, two free energies, $A_{1,2}(x) = V_{1,2}(x) - k_B T S(x)$, account for the interplay between the biofilament interaction and the channel constraints. Since molecular motors can jump between two internal states, the corresponding expression for the overall free energy drop, ΔF, must be generalized to account for these internal changes. Accordingly, the overall free energy drop must be identified from a two-dimensional particle flux, a treatment that we leave for a future study. This system is also characterized by three dimensionless parameters: $\beta \mathcal{V}_1$ and ΔS control the amplitude of the enthalpic and entropic contribution, respectively, while ω_1/ω_2 quantifies the departure from detailed balance.

C. Thermal ratchet

As a last example, we will consider a Brownian particle moving in a varying-section channel under the influence of a local temperature gradient. In the absence of entropic barriers, the transport induced by the imposed temperature gradient has been analyzed previously.[27,28] By assuming local equilibrium along the radial directions the probability distribution

function obeys[23]

$$P(\mathbf{r}, t) = p(x, t) \frac{e^{\frac{-W(\mathbf{r})}{K_B T(x)}}}{e^{\frac{-A(x)}{k_B T(x)}}}, \tag{18}$$

and the corresponding Fick-Jacobs equation reads

$$\frac{\partial}{\partial t} p(x, t) = \frac{\partial}{\partial x} \left\{ \mu(x) p(x, t) \left(T(x) \frac{\partial}{\partial x} \frac{A(x)}{T(x)} \right. \right.$$
$$\left. + V(x) \frac{\partial}{\partial x} \ln T(x) \right) + \mu(x) \frac{\partial}{\partial x} [T(x) p(x, t)] \Big\}, \tag{19}$$

where we keep the phenomenological dependence of the diffusion on the channel width through the local mobility $\mu(x) = \beta D(x)$. The overall free energy drop can be expressed as

$$\Delta F = \int_0^L \left[\frac{\partial}{\partial x} \frac{A(x)}{T(x)} + \left(\frac{V(x)}{T(x)} + 1 \right) \frac{\partial}{\partial x} \ln T(x) \right] dx, \tag{20}$$

which differs qualitatively from the one obtained for the flashing ratchet, Eq. (16). For a periodic thermal ratchet under a periodic temperature gradient, the entropic contribution, $\int_0^L \frac{\partial}{\partial x} \frac{A(x)}{T(x)} dx$, vanishes and does not contribute to ΔF. Therefore, rectification in a periodic thermal ratchet, quantified by $\Delta F = \int_0^L \frac{V(x)}{T(x)} \partial_x \ln T(x) dx$, can only develop from an interplay between the enthalpic and temperature variations.[28,29] Although both the flashing and the thermal ratchet are characterized by a multiplicative noise, their different physical origin is at the basis of this different response. For the thermal ratchet the spatial inhomogeneity affects both the amplitude of the fluctuations and the local equilibrium distribution while for the flashing ratchet the noise amplitude is regarded as an effective coarse-graining of a molecular mechanism that is decoupled from the underlying equilibrium properties of the Brownian particle. In fact, if we would (inconsistently) neglect the spatial dependence of the temperature in the equilibrium distribution of the thermal ratchet that appears in Eq. (18), we would derive a ΔF_T,

$$\Delta F_T = \int_0^L \frac{\partial_x A(x)}{T(x)} + \partial_x \ln T(x) dx \tag{21}$$

qualitatively analogous to the one obtained for the flashing ratchet, Eq. (16). A similar result, and hence the possibility of constrained-controlled rectification, is obtained if one assumes that the temperature becomes anisotropic. This corresponds to situations where the equilibration transverse to the channel is determined by a temperature that differs from the one characterizing the particle diffusion along the channel. Such situations can develop if there is an intrinsic mechanism for energy dissipation, as has been reported, e.g., in vibrated granular gases.[30]

IV. FULLY SYMMETRIC CASE

We will first consider the case of symmetric ratchet and entropic potentials, implemented for $h_2 = \lambda = 0$. Under these conditions, current rectification is not possible when entropic
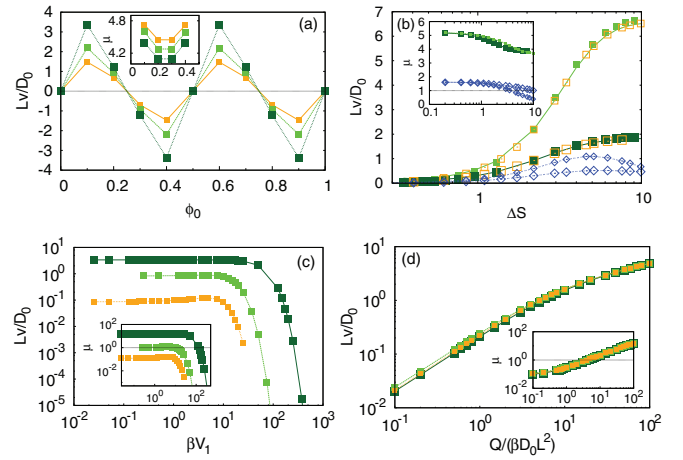

FIG. 2. Rectification of a Brownian motor moving due to a symmetric flashing ratchet in a symmetric channel. (a) Particle velocity, in units of D_0/L, being $D_0 = D_0(R = 1)$, as a function of the phase shift ϕ_0 for different values of the parameter $\Delta S = 1.73, 2.19, 2.94$ (the larger the symbol size, the larger ΔS), being $\mathcal{V}_1 = 0.2$ and $Q = 2$. (Inset) μ as a function of ϕ_0 for the same parameters. (b) Particle velocity as a function of ΔS upon variation of particle radius R (solid lines, with $h_0 = 1.25$, $h_1 = 0.2$), h_0 (solid points, with $R = 1$, $h_1 = 0.2$) or h_1 (open points, with $R = 1$, $h_0 = 1.25$) for $\phi_0 = 0.1, 0.2$ and $\mathcal{V}_1 = 0.2$, $Q = 2$ (the larger the symbol the larger ϕ_0). As a comparison the case with $\mathcal{V}_1 = 0.2$, $Q = 0.02$ and $\phi_0 = 0.1, 0.2$ (the larger the symbol the larger ϕ_0), is shown (blue diamonds). (Inset) μ as a function of ΔS for the same parameters. (c) Particle velocity as a function of the ratchet potential amplitude $\mathcal{V}_1$ for $Q = 0.02, 0.2, 2$ (the larger the symbol the larger Q), while $\Delta S = 2.94$, $\phi_0 = 0.1$. (Inset) μ as a function of ϕ_0 for the same parameters. (d) Particle velocity as a function of Q for $\mathcal{V}_1 = 0.02, 0.2, 2$ and $\Delta S = 2.94$, $\phi_0 = 0.1$ (the larger the symbol the larger $\mathcal{V}_1$).

and enthalpic forces act separately. We will show in this section that rectification may arise due to the interplay between both drivings, when they are phase shifted an amount ϕ_0.

Flashing ratchet: Figure 2(a) shows the particle current obtained by solving Eq. (15) under the steady-state condition $\dot{p}(x) = 0$. As shown in Fig. 2(a), a net particle current develops when the phase shift, ϕ_0, is not a multiple of π. Such a particle flux is the result of the interplay between confinement and the potential leading to particle rectification. In fact, Eq. (16) together with Eq. (6) clearly show that, if the channel and the ratchet are not in phase, $\phi_0 \neq 0$, the overall free energy drop, Eq. (16), is finite and a net current develops. The Fick-Jacobs equation identifies ϕ_0 and ΔS as the relevant parameters that control rectification. ϕ_0 is responsible for the spatial symmetry breaking[31] for any finite channel modulation, ΔS. A straight channel, $\Delta S = 0$, will not induce rectification because the underlying potential is symmetric. As shown in Fig. 2(b), ΔS quantifies the changes in the system geometrical properties by tuning the particle radius, R, or the channel corrugation, h_1.

Particle current varies smoothly with the other dimensionless parameters, $\mathcal{V}_1$ and Q. For example, the value of ΔS providing the maximum current is only weakly affected by a drop of Q of two orders of magnitude, as shown in Fig. 2(b). For small values of Q, the particle velocity does not increase monotonously with $\mathcal{V}_1$. While Fig. 2(c) indicates that there exists a finite value of $\mathcal{V}_1$ at which particle flux is optimal, Fig. 2(d) shows that the particle current increases monotonously with Q, leading to a monotonous increase of

the particle current. Since both the channel corrugation and the ratchet potential are symmetric, Fig. 2(a) is symmetric under inversion of the velocity and dephasing angle. Therefore, a uniform distribution of ϕ_0 will not induce any net current, but any asymmetric distribution will.

The insets of Fig. 2 display the changes of the dimensionless velocity, μ (Eq. (15)), as a function of the relevant dimensionless parameters. They show that there are regimes where confinement and the ratchet potential cooperate to induce an efficient particle rectification, $\mu > 1$, and regimes where they compete with each other, partially hindering rectification, $\mu < 1$. Both regimes depend weakly on confinement, as shown in the top panels of Fig. 2, while μ is significantly affected by the magnitude both of the ratcheting potential, $\mathcal{V}_1$, and the noise amplitude, Q. In particular, $\mu < 1$ is typical for small values of $\mathcal{V}_1$ and Q while, upon increasing both $\mathcal{V}_1$, and Q, the $\mu > 1$ regime arises. As the magnitude of $\mathcal{V}_1$ increases, μ decreases drastically and the net current eventually vanishes.

Two state model: Figure 3(a) shows that a net particle current develops when the ratchet potential and the channel corrugation are out of registry. The symmetry of the channel and rectifying potentials imply that the velocity profile is invariant if both axis of the figure are inverted; hence a uniform distribution of ϕ_0 will not induce a net current, but any asymmetric distribution will. The internal reorganization of the molecular motor as it moves along the channel allows for

qualitatively new scenarios with respect to the rectification features observed for the flashing ratchet. For example, Figs. 3(b) and 3(c) show that the particle flux can reverse its direction as ΔS and $\mathcal{V}_1$ increase, respectively, although flux reversal is more sensitive to channel corrugation. This flux reversal can be exploited to induce particle separation according to their size (due to the implicit dependence of ΔS on particle radius, R), or the differential particle response to $\mathcal{V}_1$.[32]

Although ΔS captures the essential features of net molecular motor motion, Fig. 3(b) shows separate sensitivity to the rest of the geometrical channel parameters, h_0, h_1, as well as motor size R. Such sensitivity is remarkable at smaller entropic barrier magnitudes where the confining-tuned diffusion coefficient, Eq. (8), plays a relevant role. If $h_1 \to 0$ then both the entropic barrier and the modulation of the diffusion coefficient vanish. On the contrary if R or h_0 decrease at fixed h_1, then $\Delta S \to 0$ but the modulation of the diffusion coefficient persists, allowing for rectification. As ΔS increases, the sensitivity to the separate variation of h_0, h_1, and R for the case of non-processive motors intensifies. These deviation from the geometrical dependence only through ΔS arise because the binding rate, ω_{21}, depends on the probability that the motor is close to the filament, which depends indirectly on the channel section. Hence, different channel amplitudes h_0, h_1, R, even if leading to the same ΔS, give rise to different binding rates that modulate the molecular motor velocity. This sensitivity is not present for processive motors, as observed in Fig. 3(b).

Molecular motors show a maximum current for an optimal ΔS that depends weakly on $\mathcal{V}_1$, as displayed in Fig. 3(c), while Fig. 3(d) shows that an optimum velocity, sensitive both to ϕ_0 and ΔS, can also be achieved on increasing the ratio of binding and unbinding rates, ω_{21}/ω_{12}.

V. SYMMETRIC POTENTIAL AND ASYMMETRIC CHANNEL

The channel asymmetry with respect to its transverse axis, $h_2 \neq 0$, breaks the left-right spatial symmetry along the channel longitudinal axis. Such an asymmetry leads to substantial changes in rectification with respect to the symmetric channel described earlier because now there exists a geometrically induced preferential direction for particle rectification. As in the previous case, rectification here is induced by the asymmetric confinement.

Flashing ratchet: Figure 4(a) shows that the channel asymmetry leads to asymmetric net particle current as a function of the phase shift, ϕ_0. Non-vanishing average velocities develop even when the channel and the ratchet are in registry, $\phi_0 = 0$, $1/2$, 1. Hence now a mean, non-vanishing velocity can persist for a uniform distribution of ϕ_0 as shown in the inset of Fig. 4(b). The average particle velocity in the case of a broader distribution of ϕ_0 is quite reduced with respect to the values obtained for a single fixed value of ϕ_0, see Fig. 4(b). Moreover, the average velocity in the former case in not significantly affected by the channel corrugation, while the dimensionless mobility, μ, takes values comparable to those obtained in the case of a fixed ϕ_0. The channel asymmetry also enhances the rectifying velocity magnitude,
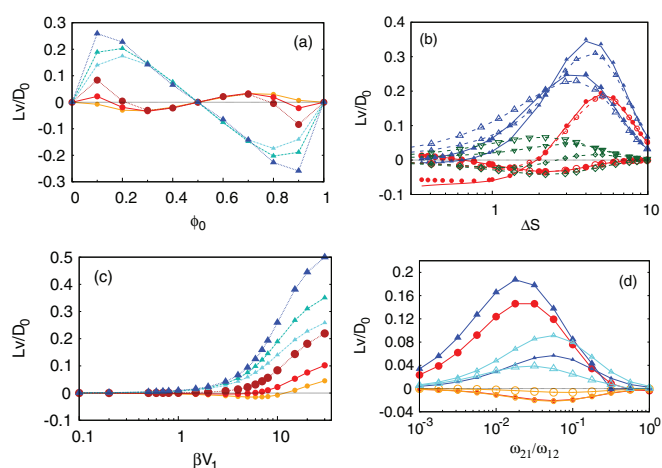

FIG. 3. Rectification of a processive (circles), non-processive (triangles) Brownian particle moving due to the two state model in a symmetric channel. (a) Particle velocity, in units of D_0/L, with $D_0 = D_0(R = 1)$, as a function of the phase shift ϕ_0 for different values of the parameter $\Delta S = 1.73$, 2.19, 2.94 (the larger the symbol size, the larger ΔS), for $\mathcal{V}_1 = 0.2$ and $\omega_{21}/\omega_{12} = 0.01$. (b) Processive (circles), non-processive (triangles) Brownian motor velocity, in units of D_0/L, as a function of ΔS upon variation of particle radius R (solid lines, for $h_0 = 1.25$, $h_1 = 0.2$), h_0 (solid points, for $R = 1$, $h_1 = 0.2$) or h_1 (open points, for $R = 1$, $h_0 = 1.25$) for $\phi_0 = 0.1$, 0.2 (larger symbols correspond to larger ϕ_0). As a comparison, the case for $\phi_0 = 0.1$, 0.2 and $\mathcal{V}_1 = 0.2$ is shown (green diamonds) (the larger the symbol, the larger ϕ_0) with $\omega_{21}/\omega_{12} = 0.01$. (The curves for $\mathcal{V}_1 = 1$ have been magnified by a factor of 5 for the sake of clarity.) (c) Processive (circles), non-processive (triangles) Brownian motor velocity as a function of the ratchet potential amplitude $\mathcal{V}_1$ for $\Delta S = 1.73$, 2.19, 2.94 (the larger the symbol, the larger ΔS) with $\omega_{21}/\omega_{12} = 0.01$. (d) Processive (circles), non-processive (triangles) Brownian motor velocity, in units of D_0/L, as a function of ω_{12}/ω_{21} for $\phi_0 = 0.1$ (0.3), open (solid) points and $\Delta S = 0.4$, 7.6 (the larger the symbol, the larger ΔS), with $\mathcal{V}_1 = 2$.
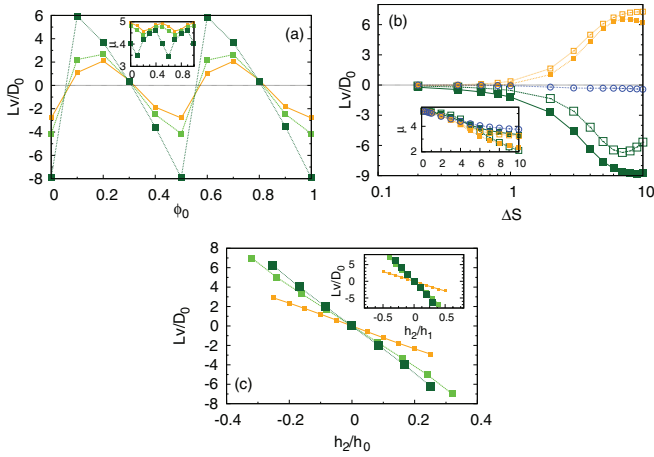
FIG. 4. Rectification of a Brownian motor moving due to a symmetric flashing ratchet in an asymmetric channel, for $h_2/h_1 = 0.25$. (a) Particle velocity, in units of D_0/L, $D_0 = D_0(R = 1)$, as a function of the phase shift ϕ_0 for different values of the parameter $\Delta S = 0.84, 2.19, 2.94$ (the larger the symbol size, the larger ΔS), with $\mathcal{V}_1 = 0.2$ and $Q = 2$. (Inset) μ as a function of ϕ_0 for the same parameters. (b) Particle velocity as a function of ΔS, varied increasing h_1 (with $R = 1$, $h_0 = 1.25$) at constant ratio $h_2/h_1 = 0.1$ (open points) and $h_2/h_1 = 0.25$ (solid points), for $\phi_0 = 0.1, 0.5$ and $\mathcal{V}_1 = 0.2$, $Q = 2$ (the larger the symbol size, the larger ϕ_0). Cyan open circles represent the average velocity obtained by a uniform distribution of ϕ_0 as a function of ΔS. (Inset) μ as a function of ΔS for the same parameters. (c) Particle velocity as a function of the channel asymmetry parameter h_2, with $\phi_0 = 0$ and $\Delta S = 1.09, 2.19$ (the larger the symbol size, the larger ΔS), for $R = 1$, $h_0 = 1.25$, $\mathcal{V}_1 = 0.2$, $Q = 2$. (Inset) μ as a function of h_2 for the same parameters.
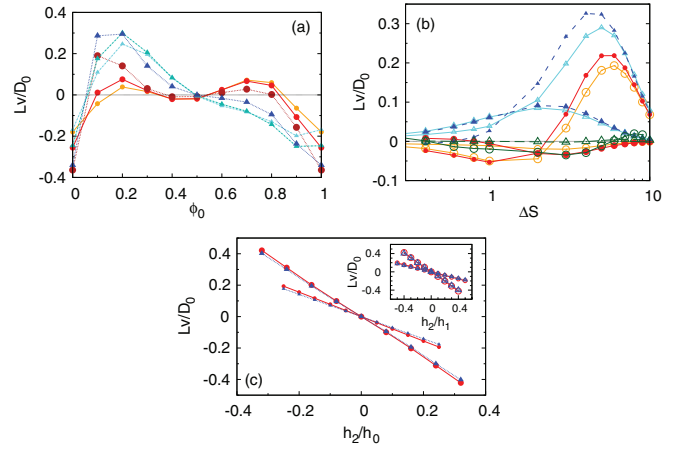
FIG. 5. Rectification of a processive (circles), non-processive (triangles) Brownian motor moving according to the two state model in symmetric ratchet and asymmetric channel, for $h_2/h_1 = 0.25$. (a) Particle velocity, in units of D_0/L, $D_0 = D_0(R = 1)$, as a function of the phase shift ϕ_0 for different values of the parameter $\Delta S = 1.73, 2.19, 2.94$ (the larger the symbol size, the larger ΔS), with $\mathcal{V}_1 = 0.2$ and $\omega_{21}/\omega_{12} = 0.01$. (b) Processive (circles), non-processive (triangles) Brownian motor velocity, in units of D_0/L, as a function of ΔS as a function of particle radius R (solid lines, with $h_0 = 1.25$, $h_1 = 0.2$) or h_1 (open points, with $R = 1$, $h_0 = 1.25$) for $\phi_0 = 0.1, 0.4$ (the larger the symbol size, the larger ϕ_0) for $\mathcal{V}_1 = 1$ and $\omega_{21}/\omega_{12} = 0.01$. Green open circles (triangles) represent the average velocity of processive (non-processive) motors obtained by a uniform distribution of ϕ_0 as a function of ΔS. (c) Processive (circles), non-processive (triangles) Brownian motor velocity as a function of h_2, being $\phi_0 = 0$, with $h_0 = 1.25$, $\mathcal{V}_1 = 0.2$, $\omega_{21}/\omega_{12} = 0.01$. The larger the symbol size, the larger the value of h_1 ($h_1 = 0.125, 0.2$).

which is almost twofold larger than the one obtained for the symmetric channel (Fig. 2(a)). The net velocity also shows a strong dependence on the channel asymmetry, ΔS. The insets of Fig. 4 show that $\mu > 1$ for all regimes considered, underlying the strong cooperative regime between the symmetric ratchet and the geometric confinement. Finally, we register a linear dependence of the particle velocity upon increasing h_2 at fixed h_1. As also shown in Fig. 4(b), the slope of the linear relation between h_2 and $\bar{v}$ depends on ΔS: increasing the entropic barrier leads to a steeper slope.

Two-state model: As for the flashing ratchet, the channel asymmetry leads to an asymmetric velocity profile upon variation of ϕ_0, as shown in Fig. 5(a). In particular, we notice that for $\phi_0 = 0$ the net velocity of processive or non-processive motors are very similar as ΔS varies (Fig. 3(a)). The asymmetric channel profile leads to an overall non-vanishing flux when averaged over the, equally weighted, values of ϕ_0. Hence, as for the flashing ratchet, we expect the channel asymmetry to provide the onset of net currents even in the case of a broader distribution of phase shifts ϕ_0. The dependence of the particle velocity on ΔS, shown in Fig. 5(b), is similar to the one obtained for the symmetric channel, Fig. 3(b), where an optimal value of ΔS is observed for both processive and non processive motors. As in the symmetric configuration, the dependence of motors' velocity on the different geometric parameters (h_1 and R) is quite well captured by the entropic barrier ΔS, although a separate sensitivity on h_1 and R persists for both processive and non-processive motors. Particle current depends linearly on h_2, as shown in Fig. 5(c). increasing the slope for larger values of ΔS.

VI. ASYMMETRIC POTENTIAL AND SYMMETRIC CHANNEL

An asymmetric ratchet potential, $\lambda \neq 0$, in the presence of a symmetric periodic channel, $h_2 = 0$, allows us to address the impact that an inhomogeneous environment has on an intrinsically rectifying Brownian ratchet. In particular, cooperative rectification modulates the particle velocity allowing for the emergence of effective particle fluxes opposing the direction of motion of the intrinsic Brownian ratchet.

Flashing ratchet: Figure 6(a) shows that the intrinsic Brownian ratchet net velocity, v_0, is strongly modulated by the channel corrugation. CBR in this case can exhibit both regimes where the average velocities exceed v_0, showing strong velocity enhancements, as well as conditions where the velocity changes sign, indicating confinement-induced flow reversal. In the latter case, particles moving against the direction imposed by the ratchet can display speeds larger than v_0. As in the case of symmetric ratchet, these effects are magnified when rising the entropy barrier ΔS, as shown in Fig. 6(b). In the presence of flux reversal, geometrical confinement leads to a mechanism for particle separation based on their size because ΔS depends both on the channel geometry and the particle size. As shown in Fig. 6(b), modulating particles size one can control and switch their velocities, offering new venues to manipulate particles and even trap them. The average particle current obtained in a disordered channel, i.e., with a uniform distribution of ϕ_0, is not much affected by the geometrical constraint.
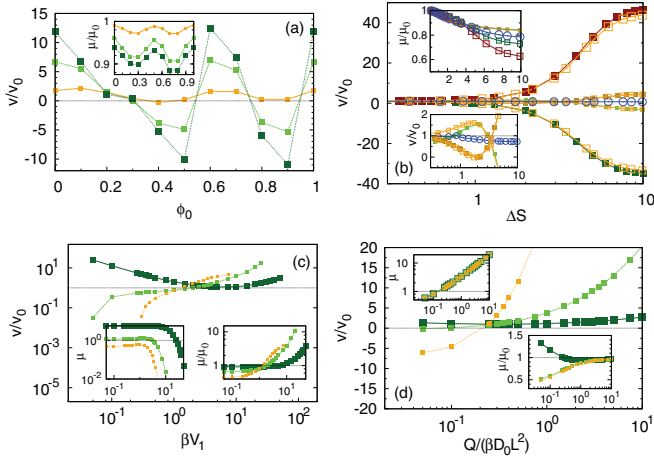
FIG. 6. Rectification of a Brownian motor moving due to a asymmetric flashing ratchet in symmetric channel. (a) Particle velocity, in units of v_0, for $\Delta S = 0$, as a function of the phase shift ϕ_0 for different values of the parameter $\Delta S = 0.84, 2.19, 2.94$ (the larger the symbol size, the larger ΔS), for $\mathcal{V}_1 = 0.2$ and $Q = 2$. (Inset) μ, in units of the dimensionless mobility, μ_0, as a function of ϕ_0 for the same parameters. (b) Particle velocity as a function of ΔS as a function of particle radius R (solid lines, with $h_1 = 1.25$, $h_2 = 0.2$), h_1 (solid points, with $R = 1$, $h_2 = 0.2$) or h_2 (open points, with $R = 1$, $h_1 = 1.25$) for $\phi_0 = 0.2, 0.3, 0.5, 0.6$ and $\mathcal{V}_1 = 0.2$, $Q = 2$ (the larger the symbol size, the larger ϕ_0). Cyan open circles represent the average velocity obtained by a uniform distribution of ϕ_0 as a function of ΔS. (Inset) μ/μ_0 as a function of ϕ_0 for the same parameters. (c) Particle velocity as a function of the ratchet potential amplitude, $\mathcal{V}_1$, for $Q = 0.02, 0.2, 2$ (the larger the symbol size, the larger Q), for $\Delta S = 2.94$, $\phi_0 = 0.1$. (Insets) μ and μ/μ_0 as a function of ϕ_0 for the same parameters. (d) Particle velocity as a function of Q. Squares for $\mathcal{V}_1 = 0.1, 1, 10$ and $\Delta S = 2.94$, $\phi_0 = 0.1$ (the larger the symbol size, the larger $\mathcal{V}_1$); triangles: $Q = 1$, $\Delta S = 1.1$, $\phi_0 = 0.5$, and $\mathcal{V}_1 = 1$. (Insets) μ and μ/μ_0 as a function of ϕ_0 for the same parameters.
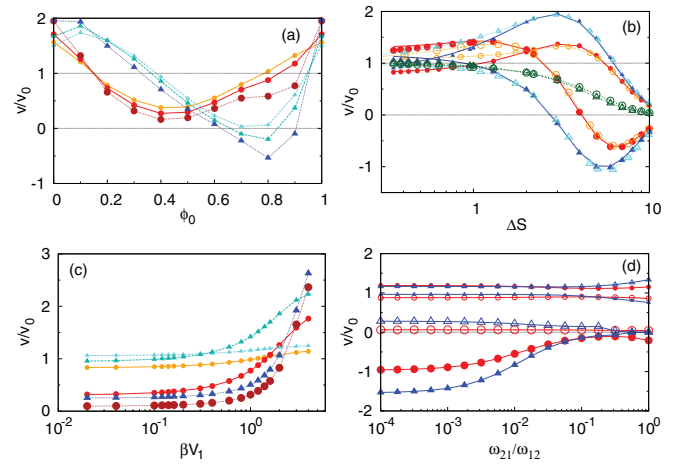
FIG. 7. Rectification of a processive (circles), non-processive (triangles) Brownian motor moving due to the two state model in symmetric channel. (a) Particle velocity, in units of v_0 as a function of the phase shift ϕ_0 for different values of the parameter $\Delta S = 1.73, 2.19, 2.94$ (the larger the symbol size, the larger ΔS), for $\Delta V_1 = 0.2$ and $\omega_{21}/\omega_{12} = 0.01$. (b) Processive (circles), non-processive (triangles) Brownian motor velocity, in units of D_0/L, as a function of ΔS and particle radius R (solid lines, with $h_0 = 1.25$, $h_1 = 0.2$), h_0 (solid points, with $R = 1$, $h_1 = 0.2$) or h_1 (open points, with $R = 1$, $h_0 = 1.25$) for $\phi_0 = 0.1, 0.9$ (the larger the symbol size, the larger ϕ_0) for $\mathcal{V}_1 = 1$ and $\omega_{21}/\omega_{12} = 0.01$. Green open circles (triangles) represent the average velocity of processive (non-processive) motors obtained by a uniform distribution of ϕ_0 as a function of ΔS. (c) Processive (circles), non-processive (triangles) Brownian motor velocity as a function of the ratchet potential amplitude $\mathcal{V}_1$ for $\Delta S = 0.4, 2, 7.6$ (the larger the symbol size, the larger ΔS) with $\omega_{21}/\omega_{12} = 0.01$. (d) Processive (circles), non-processive (triangles) Brownian motor velocity as a function of ω_{12}/ω_{21} for $\phi_0 = 0.1, 0.3$, open (solid) points and $\Delta S = 0.4, 7.6$ (the larger the symbol size, the larger ΔS) for $\mathcal{V}_1 = 10$.

The absolute value of particle current (not shown) is also very sensitive to $\mathcal{V}_1$ and Q, analogously to the results obtained for the symmetric channel (Figs. 2(c) and 2(d)). Figures 6(c) and 6(d) display strong enhancements of the net particle velocity, up to two orders of magnitude larger than v_0. These large enhancements are observed when $\mathcal{V}_1/\Delta S \ll 1$, indicating that cooperativity relies mostly on the interplay between the geometrical confinement and the position-dependent noise amplitude rather than on the asymmetric potential $V(x)$ itself.

Since the Brownian ratchet is characterized by an intrinsic rectifying velocity, v_0, it is useful to study the ratio μ/μ_0 in order to quantify the relative variation in the mobility of a CBR due to the geometrical constraints. In Figs. 6(a) and 6(b) $\mu_0 = 6.1$, hence the system takes advantage of the x-dependent free energy gradient induced by the intrinsic ratchet mechanism. The dependence of μ on $\mathcal{V}_1$ and Q is quite similar to the one observed in symmetric channels (Fig. 2): larger values of the mobility are registered for small and moderate values of $\mathcal{V}_1$ and mild and large values of Q, while for larger values of $\mathcal{V}_1$ μ drops. On the contrary, μ/μ_0 increases monotonously with $\mathcal{V}_1$ irrespectively of Q, while the dependence on Q at fixed $\mathcal{V}$ is more involved as shown in Fig. 6(d).

Two state model: Figure 7(a) displays the net velocity as a function of the dephasing between the geometric confinement and the underlying ratchet potential. Cooperative rectification now shows a strong dependence on the phase shift, ϕ_0,

leading to large velocity amplification and also to flux reversal, a feature that was not possible for symmetric channels. In fact, both processive and non-processive motors show velocity enhancement and reversal when varying the channel corrugation, ΔS, as shown in Fig. 7(b). Hence, even symmetric channels offer the possibility to control molecular motor motion according to their size, allowing for segregation and particle trapping. Interestingly, for asymmetric ratchets the entropic barrier ΔS captures even better the dynamics, as compared to the case of symmetric ratchets, and only at smaller ΔS the different behavior upon variation of h_0, h_1, and R becomes appreciable. Looking at the velocity dependence as a function of $\mathcal{V}_1$, shown in Fig. 7(c), we find a behavior similar to the one obtained for the symmetric ratchet. On the contrary, the velocity dependence upon variation of ω_{21}/ω_{12}, shown in Fig. 7(d), is very mild for smaller ΔS while for larger ΔS velocity inversion happens for smaller values of ω_{21}/ω_{12}.

VII. FULLY ASYMMETRIC CASE

When both the ratchet as well the channel left-right symmetry are broken, $\lambda \neq 0$ and $h_2 \neq 0$, all the features we have discussed previously are now present. Rather than attempting a systematic analysis of the performance of CBR in this regime, that is very rich, we will point out the basic differences with the previous cases.
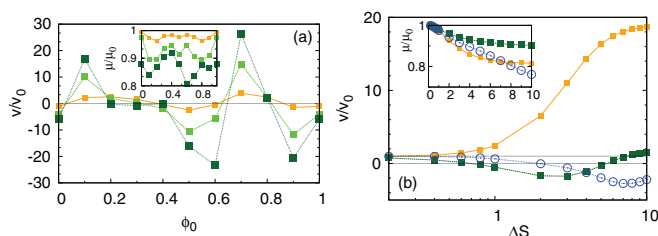
FIG. 8. Rectification of a Brownian motor moving according to an asymmetric flashing ratchet in an asymmetric channel. (a) Particle velocity, in units of the velocity, v_0, provided by the ratchet for $\Delta S = 0$, as a function of the phase shift ϕ_0 for different values of the parameter $\Delta S = 0.84, 2.19, 2.94$ (the larger the symbol size, the larger ΔS), for $\mathcal{V}_1 = 0.2$, $h_2/h_1 = 0.25$ and $Q = 2$. (Inset) μ, in units of the dimensionless mobility μ_0 as a function of ϕ_0 for the same parameters. (b) Particle velocity as a function of ΔS and h_1 (with $R = 1$, $h_0 = 0.25$) for $\phi_0 = 0.1, 0.4$, $h_2/h_1 = 0.25$ and $\mathcal{V}_1 = 0.2$, $Q = 2$ (the larger the symbol size, the larger ϕ_0). Cyan open circles represent the average velocity obtained by a uniform distribution of ϕ_0 as a function of ΔS. (Inset) μ/μ_0 as a function of ϕ_0 for the same parameters.

Flashing ratchet: As shown in Fig. 8(a), the asymmetry in both channel shape and ratchet potential lead to non-intuitive velocity variations with ϕ_0; one can identify velocity enhancement/reduction as well as velocity inversion as a function of the off-registry angle. Moreover, different values of ΔS strongly modulate the velocity dependence on ϕ_0 as shown in Fig. 8(a). Looking at the dependence of the velocity on ΔS, Fig. 8(b), we observe a strong non-monotonic response where the motor velocity, initially enhanced, is reduced by increasing ΔS until it is inverted for larger values of ΔS. As in the previous cases, we find a wide range of values of μ as well as of μ/μ_0 underlying that the sensitivity of CBRs in this scenario as a function of the changes in the geometrical constraints and ratchet parameters.

Two state model: As for the flashing ratchet case, the presence of both channel and ratchet asymmetries leads to a non trivial velocity profile upon variation of ϕ_0. Again we find here the presence of velocity enhancement, reduction or even inversion, see Fig. 9(a). Surprisingly, the velocity dependence on ΔS reminds the one obtained in the case of asymmetric ratchet in a symmetric channel. The entropic barrier,
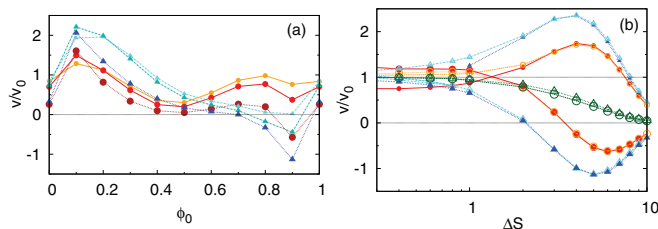

FIG. 9. Rectification of a processive (circles), non-processive (triangles) Brownian motor moving due to the two state model in an asymmetric channel. (a) Particle velocity, in units of v_0, for $\Delta S = 0$, as a function of the phase shift ϕ_0 for different values of the parameter $\Delta S = 1.73, 2.19, 2.94$ (the larger the symbol size, the larger ΔS), for $\Delta V_1 = 0.2$, $h_2/h_1 = 0.25$, and $\omega_{21}/\omega_{12} = 0.01$. (b) Processive (circles), non-processive (triangles) Brownian motor velocity, in units of D_0/L, as a function of ΔS and particle radius R (solid lines, with $h_0 = 1.25$, $h_1 = 0.2$, $H_2/h_1 = 0.25$) or h_1 (open points, with $R = 1$, $h_1 = 1.25$, $h_2/h_1 = 0.25$) for $\phi_0 = 0.1, 0.9$ (the larger the symbol size, the larger ϕ_0) for $\mathcal{V}_1 = 1$ and $\omega_{21}/\omega_{12} = 0.01$. Green open circles (triangles) represent the average velocity of processive (non-processive) motors obtained by a uniform distribution of ϕ_0 as a function of ΔS.

ΔS, captures the essential response of the confined molecular motors, even better than in the cases for which the ratchet is symmetric. Finally, also the net motors flux in a disordered channel, i.e., with equally distributed ϕ_0, has a behavior similar to the one obtained in the case of symmetric channel.

VIII. CONCLUSIONS

In this paper we have analyzed the motion of Brownian ratchets in confined media. We have shown that the interplay between the intrinsic ratchet motion and the geometrically induced rectification gives rise to a variety of dynamical behaviors not observed in the absence of the geometrical confinement. A novel effect, named cooperative rectification, arises as the net result of the overlap between the dynamic induced by the ratchet and the confinement and it is responsible for the onset of net currents even when neither the ratchet nor the geometrical constraint can rectify per se. The dynamics of the particles can be analyzed by means of the Fick-Jacobs equation. Such an approach has allowed to identify two parameters, namely, the entropic barrier ΔS an the free energy drop ΔF, that govern the overall dynamics of CBRs. On one hand, ΔF controls the onset of the cooperative rectification when $\Delta F \neq 0$. Then, cooperative rectification leads to a net current whose sign is determined by ΔF. On the other hand, ΔS accounts for the relevance of confinement in the overall dynamics when $\Delta S \neq 0$.

We have discussed when entropic confinement affects the rectification of a Brownian ratchet by contrasting physically different ratchet mechanisms. In particular, in the analysis of Brownian rectification induced by an inhomogeneous temperature profile we have clarified the relevance of the underlying mechanism breaking detailed balance. For a flashing ratchet the second moment of the longitudinal velocity of a CBR differs from the second moment associated to its transverse velocity while such an intrinsic anisotropy is lacking for the thermal ratchet. As a result, confined thermal ratchets can rectify only if there is an interplay between the asymmetric enthalpic potential and temperature gradients.

Comparing the cases of a flashing ratchet and a two-state model of a molecular motor we conclude that the novel mechanism we describe is qualitatively robust with respect to the details of the Brownian ratchet. However, the specificity of the rectification can affect both the quantitative response of a Brownian ratchet to confinement and, in some cases, even affect the qualitative behavior observed; e.g., velocity inversion can be observed increasing ΔS for processive molecular motors in a symmetric channel while velocity inversion is never observed for non-processive motors. The Fick-Jacobs approach has provided insight to understand these qualitative differences.

We have always assumed that the confining channel and the ratchet potential have the same period. If both components have different periodicities, or if one of them show irregularities (that can emerge, for example, from experimental defects in the channel build up), one can still account for the mismatch between the ratchet potential and the channel corrugation by considering that the phase shift ϕ_0, rather than having

a well defined value, is characterized by a uniform distribution. The results reported show that, in this situation a net current persists except for the fully symmetric geometry.

For asymmetric, intrinsically rectifying ratchets, we have seen that CBRs are very sensitive to corrugation and that the geometrical constraints strongly affect their motion. Controlling the corrugation of the channel one can enhance significantly the net Brownian ratchet velocity or can induce velocity inversion for all the Brownian ratchet models considered. Therefore, confinement provides a means to control particle motion at small scales. Since particles with different sizes show a differential sensitivity to the geometrical constraints, it is possible to use channel corrugation to segregate Brownian ratchets of different sizes, or even trap particles. Therefore, CBRs offer new venues to particle control at small scales.

ACKNOWLEDGMENTS

[1] R. D. Astumian, Science **917**, 276 (2010).
[2] P. Hänggi and F. Marchesoni, Rev. Mod. Phys. **81**, 387 (2009).
[3] J. L. Mateos, A. V. Arzola, and K. Volke-Sepúlveda, Phys. Rev. Lett. **106**, 168104 (2011).
[4] S.-H. Lee, K. Ladavac, M. Polin, and D. Grier, Phys. Rev. Lett. **94**, 110601 (2005).
[5] R. Balzan, F. Dalton, V. Loreto, A. Petri, and G. Pontuale, Phys. Rev. E **83**, 031310 (2011).
[6] D. V. D. Meer, P. Reimann, K. V. D. Weele, and D. Lohse, Phys. Rev. Lett. **92**, 184301 (2004).
[7] G. Thomas, J. Prost, P. Martin, and J.-F. Joanny, Curr. Opin. Cell Biol. **22**, 14 (2010).
[8] T. Hugel and C. Lumme, Curr. Opin. Biotechnol. **21**, 683 (2010).
[9] R. D. Astumian, Biophys. J. **98**, 2401 (2010).
[10] F. Jülicher, A. Ajdari, and J. Prost, Rev. Mod. Phys. **69**, 1269 (1997).
[11] P. Reimann, Phys. Rep. **361**, 57 (2002).
[12] J. M. Rubi and D. Reguera, Chem. Phys. **375**, 518 (2010).
[13] D. Reguera, G. Schmid, P. S. Burada, J. M. Rubi, P. Reimann, and P. Hänggi, Phys. Rev. Lett. **96**, 130603 (2006).
[14] P. Burada, Y. Lib, W. Rieflerb, and G. Schmid, Chem. Phys. **375**, 514 (2010).
[15] R. M. Barrer, *Zeolites and Clay Minerals as Sorbents and Molecular Sieves* (Academic, New York, 1978).
[16] C. Calero, J. Faraudo, and M. Aguilella-Arzo, Phys. Rev. E **83**, 021908 (2011).
[17] L. Dagdug, A. M. Berezhkovskii, Y. A. Makhnovskii, V. Y. Zitsereman, and S. Bezrukov, J. Chem. Phys. **134**, 101102 (2011).
[18] E. Altintas, E. Sarajlic, F. K. Bohringerb, and H. Fujita, Sens. Actuators A **154**, 123 (2009).
[19] S. Martens, G. Schmidt, L. Schimansky-Geier, and P. Hänggi, Phys. Rev. E **83**, 051135 (2011).
[20] J. F. Wambaugh, C. Reichhardt, C. J. Olson, F. Marchesoni, and F. Nori, Phys. Rev. Lett. **83**, 5106 (1999).
[21] P. Malgaretti, I. Pagonabarraga, and J. M. Rubi, Phys. Rev. E **85**, 010105(R) (2012).
[22] M. H. Jacobs, *Diffusion Processes* (Springer-Verlag, New York, 1967).
[23] R. Zwanzig, J. Phys. Chem. **96**, 3926 (1992).
[24] D. Reguera and J. M. Rubi, Phys. Rev. E **64**, 061106 (2001).
[25] P. S. Burada, G. Schmid, D. Reguera, J. M. Rubi, and P. Hänggi, Phys. Rev. E **75**, 051111 (2007).
[26] P. Reimann and P. Hänggi, Appl. Phys. A **75**, 169 (2002).
[27] N. G. van Kampen, J. Math. Phys. **29**, 1220 (1988).
[28] M. Buttiker, Z. Phys. B **68**, 161 (1987).
[29] A. Perez-Madrid, J. Rubi, and P. Mazur, Physica A **212**, 231 (1994).
[30] D. van der Meer and P. Reimann, Europhys. Lett. **74**, 384 (2006).
[31] A similar characterization has been made for a diffusing particle in contact with a temperature-position heat bath in the presence of an external conservative periodic potential.[28]
[32] In this fully symmetric regime, the velocity inversion, upon variation of ΔS, is registered only for processive motors with $\phi_0 = 0.1$.